Acquisition Techniques in Galileo AltBOC Signals

João Paulo Mateus Pires
joao.mateus.pires@ist.utl.pt

Instituto Superior Técnico, Lisboa, Portugal

October 2016

Abstract

The objective of this work is to present a complete study of the AltBOC(15,10) modulation and to describe acquisition algorithms suitable to perform a software acquisition on the Galileo E5 band signals. The thesis starts by the full description of the AltBOC modulation. Then, it is presented the minimum hardware necessary to perform the acquisition and the basic principles of acquisition. Next, the most suitable acquisition algorithms for the AltBOC modulation are presented and described. These algorithms are then analyzed in terms of acquisition time and the probability of correct detection for different C/N_0, using simulated data as close as possible the real data. All the algorithms are analyzed in conditions of Single Side Band, Double Side Band and Direct acquisition.
Keywords: GNSS, Acquisition, AltBOC, Galileo, E5 band

1. Introduction

Galileo is an ongoing project being developed by the *European Union*, *European Space Agency* and several other European organizations, whose goal is to launch a European fully functional GNSS under civil control. This system is expected to be fully operational in 2020.

The biggest improvement over the current GNSS is the availability of dual frequencies in standard services, which will make possible to have precision in positioning down to the meter, which is unprecedented in the public available services of the current GNSS.

This work is motivated by the ongoing deployment of the Galileo system. In the next years, when the system becomes operational, there will be a need to update the current GNSS receivers, so that they can benefit not only from the current GNSS signals but also from the new signals provided by the Galileo satellites.

In particular, the most promising signal that will be transmitted is the AltBOC modulated one, present in the E5 band. In theory, the AltBOC modulation can lead to formidable precision of positioning compared to the current GNSS signals, even in the presence of multipath errors. Due to the attractiveness of the AltBOC signal, also the Chinese navigation system, Beidou, plans to transmit signals with the exact same modulation [11].

Therefore, the AltBOC signal acquisition is, and will be in the next few years, one of the most interesting problems in the study of GNSS receivers.

2. Galileo E5 Signal

2.1. E5 AltBOC(15,10) Modulation

The modulation adopted for the Galileo E5 band is called E5 AltBOC(15,10), as it uses a sub-carrier frequency, f_{sub}, of 15×1.023 MHz and a code rate, R_C, of 10×1.023 MHz.

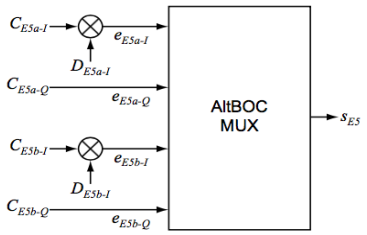

Figure 1: Modulation Scheme for the E5 Signal [4].

The E5 signal is formed by the combination of four ranging PRN codes and two data streams, according to Figure 1. The signal components are generated according to the following [4]:

- e_{5a-I} from the F/NAV navigation data stream D_{E5a-I} modulated with the unencrypted ranging code C_{E5a-I}.
- e_{5a-Q} (pilot component) from the unencrypted ranging code C_{E5a-Q}.
- e_{5b-I} from the I/NAV navigation data stream D_{E5b-I} modulated with the unencrypted ranging code C_{E5b-I}.
- e_{5b-Q} (pilot component) from the unencrypted ranging code C_{E5b-Q}.

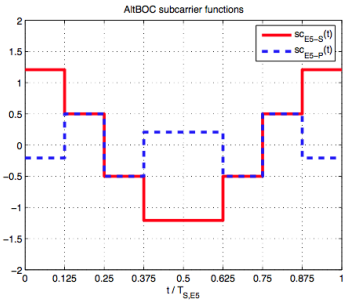

Figure 2: One Period of the Two Sub-carrier Functions Involved in AltBOC Modulation [4].

The wide-band E5 signal is generated with the AltBOC modulation, using the sub-carriers sc_{E5-S} and sc_{E5-P}, presented in Figure 2, and the components defined in Figure 1. The result is the signal $s_{E5}(t)$, which follows the expression:

$$\begin{aligned} s_{E5}(t) = & \frac{1}{2\sqrt{2}}\left(e_{E5a-I}(t) + je_{E5a-Q}(t)\right). \\ & .[sc_{E5-S}(t) - j\, sc_{E5-S}(t - T_{S,E5}/4)] \\ & + \frac{1}{2\sqrt{2}}\left(e_{E5b-I}(t) + je_{E5b-Q}(t)\right). \\ & .[sc_{E5-S}(t) + j\, sc_{E5-S}(t - T_{S,E5}/4)] \\ & + \frac{1}{2\sqrt{2}}\left(\bar{e}_{E5a-I}(t) + j\bar{e}_{E5a-Q}(t)\right). \\ & .[sc_{E5-P}(t) - j\, sc_{E5-P}(t - T_{S,E5}/4)] \\ & + \frac{1}{2\sqrt{2}}\left(\bar{e}_{E5b-I}(t) + j\bar{e}_{E5b-Q}(t)\right). \\ & .[sc_{E5-P}(t) + j\, sc_{E5-P}(t - T_{S,E5}/4)], \end{aligned} \tag{1}$$

where the dashed signal components, $\bar{e}_{E5a-I}$, $\bar{e}_{E5a-Q}$, $\bar{e}_{E5b-I}$ and $\bar{e}_{E5b-Q}$, represent the product signals:

$$\begin{aligned} \bar{e}_{E5a-I} &= e_{E5a-Q}.e_{E5b-I}.e_{E5b-Q} \\ \bar{e}_{E5a-Q} &= e_{E5a-I}.e_{E5b-I}.e_{E5b-Q} \\ \bar{e}_{E5b-I} &= e_{E5a-I}.e_{E5a-Q}.e_{E5b-Q} \\ \bar{e}_{E5b-Q} &= e_{E5a-I}.e_{E5a-Q}.e_{E5b-I}. \end{aligned} \tag{2}$$

The purpose of these product signals is solely to maintain a constant power envelope. Also, they don't carry any useful information and, therefore, are usually neglected when the signals are handled.

The PSD of the full AltBOC(15,10) modulation can be expressed as [12]:

$$\begin{aligned} G_{AltBOC(15,10)}(f) = & \frac{T_c \cos^2(\pi f T_c)}{9\cos(\frac{\pi f T_c}{3})} \\ \times & \left[\frac{4\, sinc^2(\frac{fT_c}{6})}{\cos(\frac{\pi f T_c}{3})} - sinc^2(\frac{fT_c}{12})\cos(\frac{\pi f T_c}{6})\right], \end{aligned} \tag{3}$$

where T_c is the duration of a code bit. From Equation (3) it is possible to plot the PSD of the AltBOC modulation, which is presented in Figure 3.

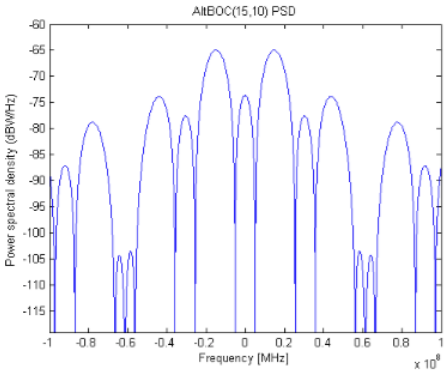

Figure 3: PSD of the AltBOC(15,10) signal [1].

In Figure 3, it can be seen that the main lobes of the AltBOC(15,10) modulation span over 50MHz. This means that a receiver capable of handling this signal needs to be able to operate with large bandwidths.

A peculiar aspect about the AltBOC is its effect on the auto-correlation function (ACF). According to [12], the modulation's ACF can be expressed as:

$$\begin{aligned} & R_{AltBOC(15,10)}(\tau) = \\ & = 8\Lambda_{T_c/6}(\tau) - \frac{16}{3}\Lambda_{T_c/6}(|\tau| - \frac{T_c}{3}) \\ & + \frac{8}{3}\Lambda_{T_c/6}(|\tau| - \frac{2T_c}{3}) - \frac{1}{3}\Lambda_{T_c/12}(|\tau| - \frac{T_c}{12}) \\ & - \frac{1}{3}\Lambda_{T_c/12}(|\tau| - \frac{3T_c}{12}) + \frac{1}{3}\Lambda_{T_c/12}(|\tau| - \frac{5T_c}{12}) \\ & + \frac{1}{3}\Lambda_{T_c/12}(|\tau| - \frac{7T_c}{12}) - \frac{1}{3}\Lambda_{T_c/12}(|\tau| - \frac{9T_c}{12}) \\ & - \frac{1}{3}\Lambda_{T_c/12}(|\tau| - \frac{11T_c}{12}), \end{aligned} \tag{4}$$

Figure 4 shows the plot of the ACF made from Equation (4).

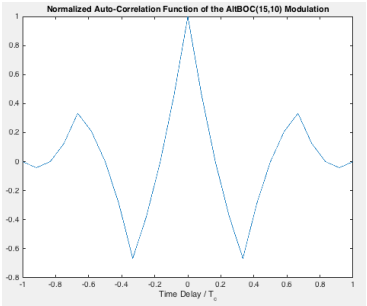

Figure 4: Normalized ACF of the AltBOC(15,10) signal.

2.2. Equivalent Modulation Type

The rather complex modulation scheme presented can be implemented using a simple Look-Up Table (LUT) to map the phase assignments.

As expressed in [4], the E5 AltBOC modulation can be described as an 8-PSK signal. Therefore, the modulated signal can, alternatively, be expressed as:

$$s_{E5}(t) = e^{j\frac{\pi}{4}k(t)} \quad \text{with} \quad k \in \{1,2,3,4,5,6,7,8\}, \tag{5}$$

where $k(t)$ defines the scattered plot number in Figure 5.

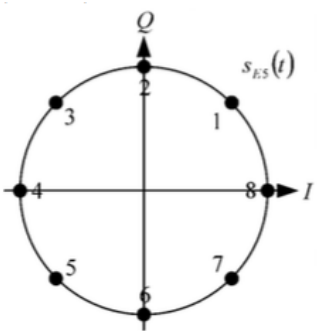

Figure 5: 8-PSK Phase-State Diagram of E5 AltBOC Signal [4].

The idea is to allocate any of the eight sub-carrier phase states and any of the sixteen (2^4) different possible states of the quadruple $e_{5a-I}(t)$, $e_{5a-Q}(t)$, $e_{5b-I}(t)$ and $e_{5b-Q}(t)$ to a phase spot in the constellation, using a LUT with 128 (8x16) different entries. Since the LUT is composed only by 128 entries, this efficient technique based on a LUT will be used for the signal generation sections on board of the Galileo satellites, obtaining a significant simplification for the necessary hardware and computational burden [9]. The complete LUT is represented in [4].

2.3. Receiver Hardware Considerations

Even though the purpose of this work is to study the E5 signal acquisition using software methods, a minimum hardware is always needed. Therefore, the hardware can not be neglected and, in this chapter, the fundamental hardware needed to achieve a correct acquisition is presented. Three types of receiver configurations are studied [9]:

- Single Band receiver: only processes one of the E5 sub-bands (E5a or E5b).
- Separate Double Band receiver: processes each one of the sidebands individually.
- Coherent Double Band receiver: this receiver processes the full-band AltBOC signal.

The single band receiver has the simplest architecture and is appropriate for simple low-cost receivers. In Figure 6 is represented a possible schematic of this type of receiver.

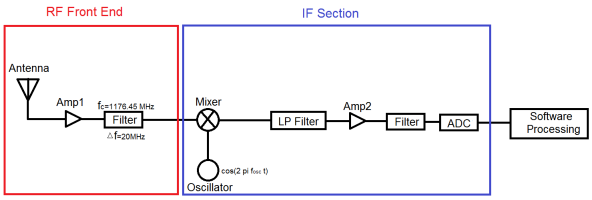

Figure 6: Architecture of a Single Band Receiver Appropriate for the Acquisition on the E5a Sideband.

The first section, corresponding to the RF front end, consists of an antenna, an amplifier and a filter. The antenna needs to cover a wide spatial angle to receive the maximum number of signals and needs to be designed in order to work correctly in the E5 band (1164-1215 MHz). A band-pass filter (centered at the chosen sideband, E5a or E5b, central frequency with a bandwidth of about 20 MHz) is used to "separate" the sideband signal from the rest of the spectrum.

The next part, corresponding to the IF (Intermediate Frequency) section, usually has an oscillator, a mixer, two filters, one or more amplifiers and an analog to digital converter (ADC). The oscillator and the mixer are used to down-convert the signal to a IF frequency. The amplifiers are designed to achieve a signal level high enough that all levels of the ADC are activated, but also low enough that no part of the ADC becomes saturated. The filter following the amplifiers is used to reduce the noise introduced by the amplifiers. Finally, the ADC quantizes and samples the analog signal in order to achieve a digital signal that can be processed in software.

The last stage of the receiver, the processing, corresponds to the software part, whose acquisition stage will be discussed in the following chapters.

The other two receiver configurations are similar to this one with some key differences:

- The separate double band receiver needs two filters after the antenna, to isolate each one of the sidebands, and it needs two IF sections (one for each sideband). For each sideband, the functional blocks of the IF section are the same as in the single band receiver.
- The coherent double band receiver differs in the entry filter: the filter bandwidth must be large enough ($\geq$ 51 MHz) to accommodate the full E5 band.

3. Acquisition Concepts

3.1. Correlation

When a Single Band receiver designed for the E5a sideband is used, the received signal can be ex-

pressed as [10]:

$$\begin{aligned} r(t) =& A.[Re\{s_{E5-a}(t-\tau)\}\cos((\omega_{IF}+\omega_d)t+\phi) \\ & - Im\{s_{E5-a}(t-\tau)\}\sin((\omega_{IF}+\omega_d)t+\phi)] \\ & + n_w(t), \end{aligned} \tag{6}$$

where s_{E5-a} are the E5a sideband components of the baseband AltBOC signal, ω_{IF} is the intermediate frequency, ω_d is the Doppler shift, τ is the time delay with respect to the transmitted signal, ϕ is the phase of the received signal and n_w is additive white Gaussian noise with power spectral density $N_0/2$.

In order to obtain a correlation value from the received signal, it is necessary to perform two steps: a carrier wipe-off and a code wipe-off. The carrier wipe-off consists in eliminating the modulation by the carrier frequency. The resulting signal frequency is the difference between the true Doppler and the receiver's estimate of Doppler. To do this, the signal from Equation (6) is multiplied by two reference signals in order to obtain in-phase and quadrature signals followed by a low-pass that filters the result. The code wipe-off is performed by multiplying each one of the in-phase and quadrature signals by a local code replica with an estimated code delay.

After both these processes are complete, the signal goes through a correlator and the output is the decision variable that is used in the decision stage.

3.2. Search Space

The acquisition step can be described as a two dimension search: in one dimension the time uncertainty (τ) is searched and in the other the frequency uncertainty (f_d), as shown in Figure 7.

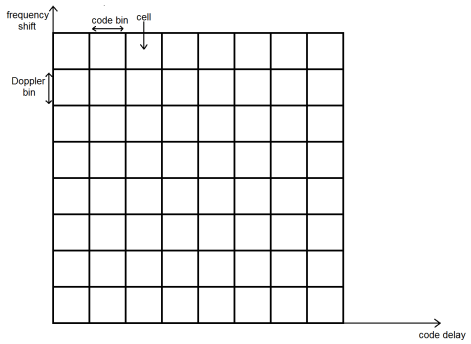

Figure 7: Representation of the Search Space.

During the acquisition stage, the correlation is performed for every single cell[1] of the search space. The size of the search space depends on the time and frequency increments. In general, for smaller increments, a better resolution and sensibility can be achieved but the size of the search increases, which means slower acquisition times.

[1] A cell is a combination of a given code and frequency bins.

3.3. Detection

After the correlation values are calculated for every single one of the search cells, the receiver needs to be able to determine if the signal from a given satellite is, or not, present. To achieve this, the receiver compares the maximum correlation value with a threshold value. If the correlation value is higher than the threshold, the signal is considered present, otherwise it is considered missing.

To set the threshold limit, a value for the false alarm probability (P_{fa}) is chosen, and the corresponding threshold is set on the basis of the PDF of the correlator output when there is no signal present. The threshold value is given by, where T_{int} is the coherent integration time:

$$V_t = \sqrt{-2N_0.T_{int}ln(P_{fa})}. \tag{7}$$

The noise power spectral density, N_0 ,needs to be estimated, and that can be done using a C/N_0 estimator. The most well-known method to estimate the C/N_0, in GNSS, is the Narrow-Wideband Power Ratio method, described in [3]. This method evaluates the total power of the correlation process at two different noise bandwidths: a Wide-Band Power (WBP_k) measurement taken over the noise bandwidth $\frac{1}{T_{int}}$; and a Narrow-Band Power NBP_k) measurement taken over the noise bandwidth $\frac{1}{M.T_{int}}$, where M is a positive integer [5].

3.4. Coherent Integration

The coherent integration consists on performing summations in a way that that different correlation samples are averaged. If more correlations samples are considered, since the noise has zero mean, the noise influence on the correlation is reduced, while the signal contribution is increased. For the acquisition of E5 signals, the coherent integration time can not exceed 1ms to avoid the bit transitions caused by the secondary code.

3.5. Non-coherent Integration

Another way to improve the correlation output is to use non-coherent integrations. This integration differs from the one presented in the previous section, as it sums the results after the correlator output. This means that not only the signal power but also the noise power is increased.

4. Acquisition Methods

4.1. Categorization of the Acquisition Methods

Due to the characteristics of the E5 AltBOC signal, there are multiple ways the acquisition can be processed. Below, the most common methods for a search strategy based acquisition are presented [11].

- Single Sideband Acquisition (SSB). This method only uses one of the sidebands to perform the acquisition.
- Double Sideband Acquisition (DSB). Here the correlation results are calculated individually for each sideband and then non-coherently combined.
- Full-band Independent Code Acquisition (FIC). In a FIC method, a locally generated individual code with the corresponding sub-carrier is multiplied with the received signal, without the necessity to filter one of the sidebands.
- Direct AltBOC Acquisition. In this method, the reference signal generator employs a LUT to combine all four signal components. The individual sub-carriers do not need to be generated and combined with the spreading codes, as the LUT essentially maps the sub-carrier phase points.

4.2. Categorization of the Search Strategies

The main difference between acquisition algorithms is in how the grid is searched. This search can be performed in a variety of ways, which are introduced next [1].

- Serial Search. In a serial search method, the cells are searched sequentially and every single cell of the grid is searched individually. This is the most basic method and it is used as a benchmark in algorithm comparison [11].
- Parallel Frequency Search. Here all the frequency bins are tested at the same time, which leaves only the code delays to be searched.
- Parallel Code Search. In this method, a simultaneous search is performed on the code delays.
- Double Parallel Search. This type of algorithm simultaneously searches all the frequency bins and all the code delay bins, which means that it determines the correlation values for the whole search grid in one iteration.

4.3. SSB/DSB Acquisition Algorithms

In this section, the most appropriate algorithms for SSB and DSB acquisition are presented. The methods shown are only exemplified for the SSB acquisition, as these two types of acquisition are in all ways similar. The only difference lies in the fact that the correlations need to be calculated twice (one for the E5a and another for the E5b sidebands) and these results to be non-coherently combined. Also, the examples provided are shown for the acquisition on the E5a sideband, but they are also valid for the E5b sideband, with the respective parameters.

4.3.1 Classical/Serial Acquisition

The classical acquisition is the most basic acquisition scheme there is and it is described in a variety of references, such as [6]. This algorithm can be classified as a serial search algorithm as the correlation output is calculated for each cell individually. The acquisition scheme is shown is figure 8.

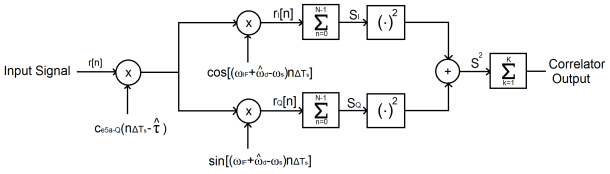

Figure 8: Architecture of the Serial Acquisition Algorithm for a Single Channel.

In this algorithm, the correlation is performed as presented in part 3. At first, the code wipe-off is done by multiplying the incoming signal by a local code replica. Then, the carrier wipe-off is done by multiplying the signal by two sinusoidal generated signals, which result in in-phase and quadrature signals independent of the carrier frequency and the code delay. The correlation results are then summed over a coherent integration time of 1ms. After the envelope detector, the results are then non-coherently combined over an interval of K times the primary code period.

After the correlation outputs are determined for every single cell of the search grid, the maximum correlation value is taken and compared to a threshold, which determines if the signal is or not present.

4.3.2 Parallel Acquisition in Frequency Domain

This algorithm, as the name suggests, performs a parallel search in the frequency domain and its scheme can be seen in Figure 9.

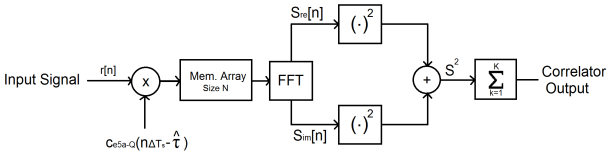

Figure 9: Architecture of the Parallel Acquisition in Frequency Domain Algorithm.

The first part of the method consists in a code wipe-off, which is done in the same way as the classical acquisition. However, the carrier wipe-off is not performed. Instead, it is replaced by a *Fourier Transform*. This transformation changes the time domain data into frequency domain data. When the local generated code is aligned with the input data, the squared output of the transformed data shows a

distinct peak, located at the index that corresponds to the frequency of the IF plus the Doppler shift. The envelope detector and the detection stage are in all similar to the previous algorithm.

The resolution that this algorithm can achieve is related to the number of FFT points. This number of points is directly related to the sampling frequency and the coherent integration time. The frequency resolution is then equal to [6]:

$$\Delta f_d = \frac{f_s}{number of samples} = \frac{f_s}{T_{int} \times f_s} = \frac{1}{T_{int}}. \quad (8)$$

4.3.3 Parallel Acquisition in Time Domain

This method has the search parallelized in time domain. To achieve this, it uses some *Fourier Transform* properties to obtain a circular correlation and its scheme is presented in Figure 10.

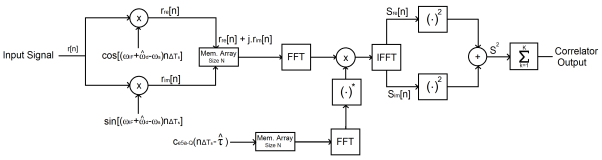

Figure 10: Architecture of the Parallel Acquisition in Time Domain Algorithm.

This solution can be considered as an alternative to the classical implementation, that produced the same results just performing the correlation by means of FFT's [6], which makes the acquisition faster.

4.3.4 Double Block Zero Padding Transition Insensitive (DBZPTI)

The DBZPTI method can be classified as double parallel search. The full description of the algorithm is presented in [7] and it summarizes the method in five steps:

1. *Pre-processing of the incoming signal.* The incoming signal is converted to baseband through a multiplication by a sinusoidal at IF. The local sinusoidal does not try to compensate the incoming Doppler frequency. Then, the samples are split into 2M blocks of equal length. Each block contains the same number of samples (N). The M value depends on the integration time and on the expected Doppler frequency and can be expressed as $M = 2f_{max} \times T_{int}$, where f_{max} corresponds to the maximum foreseeable Doppler shift. After that, each two adjacent blocks of the received signal are combined to form a block of samples.

2. *Local replica code.* M blocks of the local spreading code are generated. Each block is zero-padded, this means that samples of value 0 are appended to each block. So the local code blocks have 2N samples as the incoming signal blocks.

3. *Partial circular correlation.* Each 2N-sample block of incoming signal is circularly correlated with the corresponding first zero-padded code block of the local replica. Due to the zero padding of the local code blocks, only the first half of the resulting correlation function is preserved. The resulting matrix has dimensions of MxN and the N points represent a partial correlation of length $\frac{T_{int}}{M}$ ms at N possible delays.

4. *Circular correlation for all delays.*The incoming signal blocks are shifted one block and circular correlated with the unchanged local code blocks. This step is performed M times, for all the incoming signal combination of two blocks that correspond to each code delay. This results in M MxN matrices, that after being concatenated result in a single matrix with Mx(N×M) dimensions.

5. *Zero padding and FFT application.* The resulting matrix is zero-padded by a chosen value. According to [7], the best value corresponds to 4M. Finally, an FFT is performed for each column, one by one, which is representative of every code delay. The resulting matrix consists on the search space with all correlation values already determined.

4.4. Exploiting Secondary Codes Properties to Increase Acquisition Performance

The E5 acquisition has its T_{int} limited to 1ms. In this section, a method [11] is presented that allows the use of coherent times equal to $T_{int} = N_c.T_p$, where N_c is the number of primary code periods chosen to be part of the coherent integration. Other advantage of this method is that the secondary code acquisition is performed simultaneously to the primary code acquisition, using the characteristic length (CL) concept. This concept consists in the minimum number of bits a partial sequence must have to reconstruct the entire bit sequence.

The coherent accumulation is performed by using the knowledge of the secondary code. The coherent integration is continued for the desired duration and the decision statistic is found by taking the maximum out of all correlation values, which corresponds to the best approximation of the correct secondary code phase. Figure 11 shows the full architecture of the proposed algorithm.

The algorithm can be divided in five major parts:

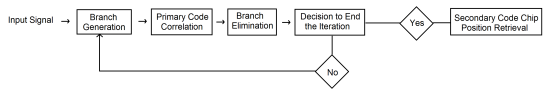

Figure 11: Architecture of the Proposed Algorithm.

1. Branch generation. In this step, the branches that contain all possible secondary code hypotheses are generated. The branches are generated following an evolutionary tree as described in [2]. Each millisecond of input data is multiplied either by the *zero bit* or the *one bit* (+1 and -1, respectively), as dictated by the corresponding branch value.

2. Primary Code Correlation. The primary code correlator performs the correlation of the input signal with local primary code replica. In each iteration, the correlation is performed over the first i milliseconds of data for each one of the branches present in the evolutionary tree. Only the maximum output for each branch is saved during this step.

3. Branch Elimination. The branch elimination logic examines all the hypotheses outputs, corresponding to each one of the branches. The criterion for the branch elimination is a lower correlation value relative to other branches.

4. Decision to End the Iteration. If $N_c < \text{CL}$, there are two choices: either the iterations are continued until, at least, the corresponding CL number of secondary bits are determined or the process stops and the secondary code shift is acquired in a different way. If $N_c > \text{CL}$, the integration is performed either until a correlation value exceeds the decision threshold or until the iteration number exceeds N_c.

5. Secondary Code Chip Position Retrieval. The secondary code hypotheses that wins corresponds to a sub-sequence within the complete secondary code. A search needs to be made in the larger sequence to determine the index of the shift.

4.5. FIC Acquisition Algorithm

4.5.1 Sub-carrier Phase Cancellation (SPC) Method

The idea behind the SPC technique is to get rid of the sub-carrier signal, the same way it is done for the carrier component. To achieve this, in addition to the local in-phase and quadrature signals used to perform the carrier wipe-off, it is necessary to generate an in-phase and a quadrature sub-carrier signals. The expression for the local in-phase sub-carrier signal, r_I, and quadrature sub-carrier signal,r_Q, are as follows [8]:

$$\begin{aligned} r_I &= c(t-\hat{\tau}).sc(t-\hat{\tau}) \\ r_Q &= c(t-\hat{\tau}).sc(t-\hat{\tau}-\frac{T_{sc}}{4}), \end{aligned} \tag{9}$$

where $c(t)$ can correspond to the primary code of any of the four channels. The method architecture is shown in Figure 12.

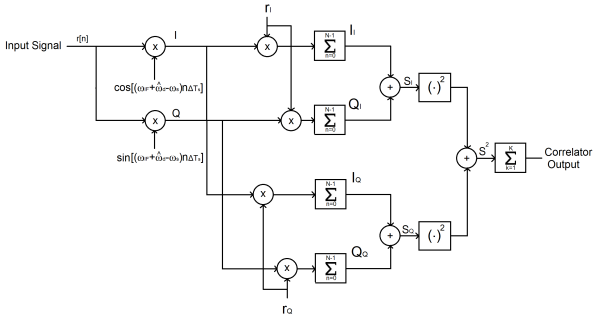

Figure 12: Architecture of the SPC Algorithm.

4.6. Direct Acquisition Algorithms

The acquisition on the full E5 band is performed in a similar way to the acquisition of a single band. However, there are some major differences. First of all, the sampling rates used need to be significantly higher, even though it makes possible to achieve better time resolution, it leads to higher computational burden, and therefore, slower acquisition times. In order to decrease the high acquisition time, it is proposed in [9] the progressive acquisition technique. Here, the input signal is down-sampled to a lower sampling rate (about 2 samples/chip [9]), so that the acquisition technique obtains an initial rough estimate of the code delay and Doppler shift. After that, the acquisition is performed for the regular sampled signal, but only around the cell that achieved the largest correlation value, increasing the resolution to the appropriate level.

Also, the code wipe-off needs to be performed in a different way. Instead of being performed for a single primary code, it needs to executed for the full modulation. To do this, the local replica is generated using the LUT approach, as to combine all four signal components. In order the eliminate the influence of the data bits, there is the need to generate four different replicas to emulate which one of the data bit combinations.

4.7. Transition to Tracking

During the acquisition, the receiver estimates both the code delay and the frequency shift of the received signal. The next stage of the receiver (tracking) requires a lock into a code loop, called Delay Locked Loop (DLL), and a carrier loop, called

Phase Locked Loop (PLL) to correctly track the signal from a given satellite. A transition stage is required between these two stages because of two issues: the secondary code phase must also be known and the estimated parameters may not have the required resolution.

To solve the first issue, after the primary code is acquired, the secondary code chips can be demodulated, by checking the signal of a correlation value in a given secondary code chip, and stored in a vector. The secondary code synchronization can then be obtained, performing a circular correlation between the vector with the estimated chips and a local replica of the secondary code [9]. Conventional GNSS receivers solve the second problem by using a *convergence phase*, where the carrier loop is a Frequency Locked Loop (FLL), to refine the frequency estimation and to allow the successive phase lock (PLL) and the DLL to work in a coarse configuration to tolerate the initial code phase errors.

5. Performance Analysis

5.1. Signal Generation

The generated signals were produced using a script implemented in the MATLAB language. These signals are generated as if they they are the output of the Analog-to-Digital Converter and they have a code delay and a frequency shift equal to $f_{IF} + f_D$ introduced to simulate the effects of the code phase and the intermediate and Doppler frequencies. Finally, an *Additive White Gaussian Noise* (AWGN) channel is simulated, by adding, to the signal samples, a Gaussian noise with zero mean and variance defined by the chosen SNR, or the corresponding C/N_0 at the input of the acquisition step.

5.1.1 Carrier-to-Noise Density Ratio

In order to obtain results that are as similar as possible as those obtained using real signals, a proper choice of the C/N_0 must be made. According to [4], the minimum received power on ground of the Galileo signals is $P_{sig} = -155dBW$ for the E5 band. Knowing that the power spectral density of the input noise, N_0, at a typical GNSS receiver is equal to 7.81×10^{-21} W/Hz, it can be assumed that the standard C/N_0 is equal to:

$$C/N_0 = 46 \text{ dB.Hz.} \tag{10}$$

5.2. Results Comparison

5.2.1 Mean Acquisition Time

The mean acquisition time (MAT) is related to the number of bins in the search space that need to be looked at and to the time it takes to analyze each one of the cells. So, the acquisition time is equal to:

$$\begin{aligned} &\text{MAT} \\ &= \text{number of cells} \times \text{time needed to search 1 cell.} \end{aligned} \tag{11}$$

The time needed to perform the acquisition not only depends on the algorithm but also on the hardware that processes the data. So, to eliminate the influence of the hardware, the time results are normalized to a reference. The reference chosen is the time it takes to perform acquisition of a single channel using the classical algorithm. The time results for the diverse algorithms were obtained by averaging 1000 different measurements and are presented in Table 1.

Algorithm	SSB	DSB	Direct
Classical	1	2.004	63.692
Parallel search in frequency	0.0290	0.0440	4.3518
Parallel search in time	5.420×10^{-5}	1.008×10^{-4}	2.928×10^{-3}
DBZPTI	3.486×10^{-5}	9.863×10^{-5}	1.442×10^{-3}

Table 1: Normalized MAT for all the studied algorithms.

From Table 1, it can be seen that the DBZPTI algorithm is the method that achieves the fastest acquisition times, having a slight advantage over the parallel search in time domain, while the classical method performs the slowest acquisition. Also, there is a considerable increase in the acquisition times when the direct acquisition is performed, independently of the algorithm considered. This increase is not only due to the increase in the number of signal channels acquired but also due to the increased sampling rates used, to the need to map the modulation using the LUT implementation and to the need to repeat the correlation process four times, so that the influence of the navigation bits is neglected.

5.2.2 Sensitivity Results

The algorithms performance was analyzed for a variety of C/N_0 and a relation between the probability of correct detection and the C/N_0 of the received signal was obtained. The probability of detection was determined by checking how many of the correlation values of the known to be present signal exceeded the set threshold. The threshold was determined for a probability of false alarm: $P_{fa} = 10^{-2}$. The results were obtained for a non-coherent integration time equal to ten primary code periods (K=10) and are shown in Figure 13.

As it can be seen from Figure 13, there is little difference between the sensitivity of the algorithms. The major difference lies on how and which signals are acquired, where the direct acquisition clearly outperforms both the SSB and DSB acquisitions.

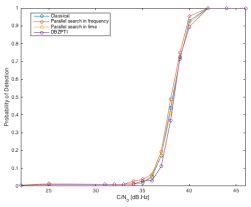

(a) SSB

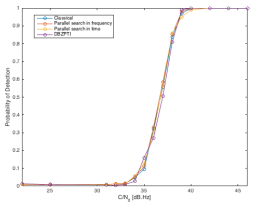

(b) DSB

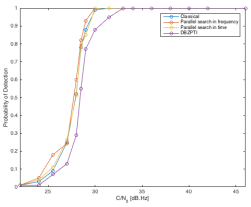

(c) Direct

Figure 13: Sensitivity comparison of the different algorithms.

5.3. Analysis on the Integration Time

In this section, a study on the effect of the integration time in acquisition performance is made. The study is performed solely for the acquisition of a single pilot channel using the DBZPTI method, since this method proved to be the fastest while presenting similar sensitivity to the other methods.

Figure 14 shows the detection probability versus the C/N_0 for one acquisition channel using a variety of non-coherent integration times (K primary code periods) with $T_{int} = 1$ ms (Figure 14(a)) and a variety of T_{int} for $K = 1$ (Figure 14(b)).

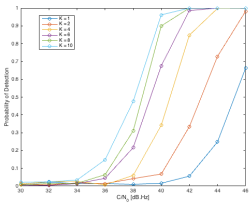

(a) Non-coherent Integration

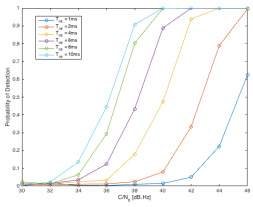

(b) Coherent Integration

Figure 14: Probability of detection versus C/N_0 using one channel acquisition.

From the analysis of Figure 14, it can be seen that, as expected, the acquisition achieves better results when the coherent integration is performed instead of non-coherent one. However, unlike the implementation of the non-coherent combination which can be done directly, to be able to use coherent integration times superior to 1 ms, it was necessary to implement to algorithm described in section 4.4. Figure 15 shows the comparison of the acquisition times for the variation of T_{int} and K, normalized to the time it takes to perform the acquisition using 1 ms of data.

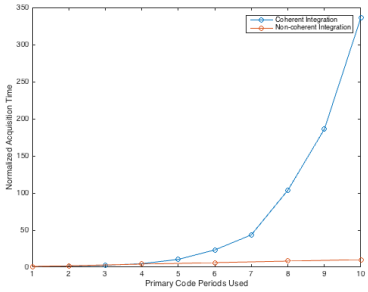

Figure 15: Acquisition time comparison between coherent and non-coherent combining.

From Figure 14, it is verified that an increase in the coherent integration interval increases the acquisition time exponentially, unlike the increase in the number of non-coherent combinations which increases the acquisition time linearly. This difference makes it that, when the data used has length higher than 4 ms, the acquisition time is much slower when coherent combining is used, as evidenced in Figure 14. This difference in time can be justified by implementation of the algorithm, which has to perform the correlation several times corresponding to each branch, and to the increased number of data, which increases the length of the Fourier transforms.

6. Conclusions

In part 2, the AltBOC modulation was presented. There, it was found that the AltBOC modulation brings many upsides but also presents many challenges in the acquisition process, such as the complexity in implementation and multi-peak autocorrelation function, that make performing the acquisition in a short time a very challenging task.

Parts 3 and 4 present the steps it takes to perform a correct acquisition. The conclusion here is that the acquisition is a complex process that can be performed in a variety of ways, each one presenting different results. In particular, the search space can be searched in a serial way or the search can be parallelized to achieve faster times. Additionally, the AltBOC modulation allows the acquisition to be performed not only for the full modulation but also for isolated components in order to achieve a faster speed.

In part 5, an analysis is done in terms of the acquisition time and the probability of correct detection for different C/N_0 for the algorithms described in part 4. The major conclusions in this chapter were:

- The difference in sensitivity is negligible when comparing the different algorithms. The major difference resides on which signals are acquired,

being the direct acquisition the clear winner.

- The time of acquisition changes drastically with the algorithm used. The faster algorithms are the ones which parallelize the search space. In particular, the faster one is the DBZPTI which performs a two-dimension parallelization. There is also a big increase in acquisition time in the direct acquisition when compared to the SSB and DSB acquisition.

- The coherent combination produces better results compared to the non-coherent combination for the same data duration. However, due to the signal characteristics, the time it takes to perform the coherent integration, specially for large integration durations, is also much higher than the time needed for the non-coherent integration.

- Performing the secondary code acquisition simultaneously with the primary code acquisition is not a good practice (unless the signal requires the use of large coherent integration times), since it leads to a considerable increase in the acquisition time. Therefore, the secondary code acquisition should be performed after the primary code is already acquired.

To sum it up, the DBZPTI algorithm was found to be the most appropriate algorithm since it presents a sensitivity comparable with the other algorithms, but at the same time exhibits time results unmatched by them. Additionally, it was found that the SSB acquisition is the fastest but presented the worst sensitivity, therefore, it is suitable for fast applications where good carrier to noise ratios are expected. On the other end, it was concluded that the direct acquisition presents the best sensitivity results in exchange for a big increase in time spent; therefore it should only be used when the noise levels are expected to be high or when the SSB is not capable of detecting the incoming signals.

An idea for a future work is to test the algorithms and methods implemented in this thesis using real data instead of simulated data. Even though there was an effort to emulate the characteristics of real data captured by a real receiver, some important issues were neglected, such as the finite number of bits in the analog-to-digital converter and the existence of error sources that can quickly vary the noise values of the signals. Only after being tested by real data that it is safe to say that the proposed methods are suitable to be used in day-to-day applications.

References

[1] P. A. M. Boto. Analysis and development of algorithms for fast acquisition of modern GNSS signals. Master's thesis, Instituto Superior Técnico, 2014.

[2] G. E. Corazza, C. Palestini, R. Pedone, and M. Villanti. Galileo primary code acquisition based on multi-hypothesis secondary code ambiguity elimination. *Proceedings of the 20th International Technical Meeting of the Satellite Division of The Institute of Navigation, Fort Worth, United States*, pages 2459 – 2465, September 2007.

[3] A. V. Dierendonck. *Global Positioning System: Theory and Applications*, volume 1, chapter 3. American Institute of Aeronautics and Astronautics, 1996.

[4] European Union. *European GNSS (Galileo) Open Service: Signal In Space Interface Control Document*, 2015.

[5] E. Falletti, M. Pini, and L. L. Presti. Low complexity carrier-to-noise ratio estimators for GNSS digital receivers. *IEEE Transactions on Aerospace and Electronic Systems*, 47(1):420–437, January 2011.

[6] M. Fantino. *Study of Architectures and Algorithms for Software Galileo Receivers*. PhD thesis, Politecnico di Torino, 2006.

[7] M. Foucras, O. Julien, C. Macabiau, and B. Ekambi. An efficient strategy for the acquisition of weak Galileo E1 OS signals. *European Navigation Conference, Vienna, Austria*, April 2013.

[8] V. Heiries, D. Roviras, L. Ries, and V. Calmettes. Analysis of non ambiguous BOC signal acquisition performance. *Proceedings of the 17th International Technical Meeting of the Satellite Division of The Institute of Navigation, Long Beach, United States*, pages 2611 – 2622, September 2004.

[9] D. Margaria. *Analysis of Receiver Architectures, Acquisition Strategies and Multipath Mitigation Techniques for the E5 AltBOC Signal*. PhD thesis, Politecnico di Torino, 2007.

[10] F. D. Nunes. AltBOC receivers. IST, 2016.

[11] N. C. Shivaramaiah. *Enhanced receiver techniques for Galileo E5 AltBOC signal processing*. PhD thesis, University of South Wales, 2011.

[12] F. M. G. Sousa and F. D. Nunes. New expressions for the autocorrelation function of BOC GNSS signals. *Navigation, Journal of the Institute of Navigation*, 60(1):1–9, March 2013.